Available online at www.sciencedirect.com
ScienceDirect
International Journal of Heat and Mass Transfer 51 (2008) 2368–2376
International Journal of HEAT and MASS TRANSFER
www.elsevier.com/locate/ijhmt

Orientation effect on natural convective performance of square pin fin heat sinks

Ren-Tsung Huang [a], Wen-Junn Sheu [a,*], Chi-Chuan Wang [b]

[a] Department of Power Mechanical Engineering, National Tsing Hua University, 101, Section 2, Kuang Fu Road, Hsinchu 300, Taiwan
[b] Energy and Environment Research Laboratories, Industrial Technology Research Institute, Hsinchu 310, Taiwan

Received 13 October 2006; received in revised form 14 August 2007
Available online 23 October 2007

Abstract

Experiments are carried out on natural convection heat transfer from square pin fin heat sinks subject to the influence of orientation. A flat plate and seven square pin fin heat sinks with various arrangements are tested under a controlled environment. Test results indicate that the downward facing orientation yields the lowest heat transfer coefficient. However, the heat transfer coefficients for upward and sideward facing orientations are of comparable magnitude. Depending on the fin structure, the performance of these two orientations shows a competitive nature. It is found that the sideward arrangement outperforms the upward one for small finning factors below 2.7, beyond which the situation is reversed. In addition, with the gradual increase in the finning factor, the performance of sideward arrangement approaches that of downward arrangement. Aside from the finning factor, the heat sink porosity has a secondary effect on the pin fin performance. The comparison among three orientations shifts in favour of upward and sideward arrangements with raising the heat sink porosity in consequence of reducing the flow resistance. The optimal heat sink porosity is around 83% for the upward arrangement and is around 91% for the sideward arrangement. In particular, the addition of surface is comparatively more effective for the downward arrangement whereas it is less effective for the sideward arrangement. This argument is supported by showing that the augmentation factor, defined as the heat transfer of a heat sink relative to that of a flat plate, is around 1.1–2.5 for the upward arrangement, around 0.8–1.8 for the sideward arrangement, and around 1.2–3.2 for the downward arrangement.

Keywords: Natural convection; Orientation effect; Square pin fin heat sink

1. Introduction

Natural convection from heat sinks has long been utilized for the thermal management of low-power-density devices. With the features of high system reliability, free of maintenance, and zero power consumption, this cooling technique plays an important role in the electronic cooling industry and has attracted considerable researches for decades. Sparrow and Vemuri [1] studied the fin orientation and the effects of fin population on natural convection/radiation heat transfer from pin fin arrays having a pin diameter of 6.35 mm and a pin height of 25.4 mm with a population density ranging from 0.31 to 1.33 pins/cm^2. Their results revealed that the upward facing orientation yielded the highest heat transfer rates, followed by the sideward facing and the downward facing ones. For the optimal fin population subject to practical values of Rayleigh number, the heat transfer rates for upward arrangement were about 15% higher than those for sideward arrangement and were about 20% higher than those for downward arrangement. Zografos and Sunderland [2] investigated the heat transfer performance of inline and staggered pin fin arrays in natural convection and concluded that the inline arrays generally yielded higher heat transfer rates than the staggered ones. In addition, their investigation showed little influence of inclination when the inclination angle was less than 30° from the vertical. Aihara et al. [3] tested a total of 59 arrays with a population density of 1.08–

* Corresponding author. Tel.: +886 3 5162099; fax: +886 3 5722840.
E-mail address: wjsheu@mx.nthu.edu.tw (W.-J. Sheu).

0017-9310/$ - see front matter © 2007 Elsevier Ltd. All rights reserved.
doi:10.1016/j.ijheatmasstransfer.2007.08.014

Nomenclature

A	surface area, m^2
Gr	Grashof number, dimensionless
g	gravity, $m\,s^{-2}$
H	fin height, mm
h	convective heat transfer coefficient, $W\,m^{-2}\,K^{-1}$
k	thermal conductivity, $W\,m^{-1}\,K^{-1}$
L	base plate edge, m
Nu	Nusselt number, dimensionless
Pr	Prandtl number, dimensionless
Q	rate of heat transfer, W
Ra	Rayleigh number, dimensionless
S	pin spacing, mm
S_p	pin edge, mm
T	temperature, °C
V_f	fluid volume in heat sink, m^3
V_{ff}	fluid volume plus fin volume in heat sink, m^3

Greek Symbols

α	thermal diffusivity of air, $m^2\,s^{-1}$
β	coefficient of thermal expansion of air, K^{-1}
ε	radiative emissivity, dimensionless
η_0	overall fin efficiency, dimensionless
θ	rotated angle relative to upward arrangement, radian
λ	thermal conductivity of air, $W\,m^{-1}\,K^{-1}$
μ	dynamic viscosity of air, $kg\,m^{-1}\,s^{-1}$
ν	kinematic viscosity of air, $m^2\,s^{-1}$
ξ	augmentation factor, dimensionless
σ	Stefan–Boltzmann constant, $W\,m^{-2}\,K^{-4}$
ϕ	heat sink porosity, dimensionless
ψ	finning factor, dimensionless

Subscripts

a	ambient
b	base plate
C	convection
Exp.	experiment
f	film
fp	flat plate
hs	heat sink
L	characteristic length
pred	prediction
R	radiation
t	total
1	surface 1
2	surface 2
3	fin surface
4	surroundings

Superscript

—	average quantity

10.58 pins/cm^2. By introducing the modified Nusselt and Rayleigh numbers, an empirical correlation which characterized the heat transfer performance of round pin fin arrays was established. Fisher and Torrance [4] presented the analytical solutions relevant to the limits of free convection for pin fin cooling. They suggested that the design of pin fin heat sink could be optimized by properly choosing the pin fin diameter and the heat sink porosity. For conventional heat sinks, the minimum thermal resistance was about two times greater than that in an ideal limit according to the model of inviscid flow with idealized local heat transfer. Park et al. [5] adopted a commercial finite-volume computational fluid dynamic code with the sequential linear programming method and weighting method to obtain an optimal design of plate heat exchangers with staggered pin arrays for a fixed volume. The flow and thermal fields were assumed to be a periodically fully developed flow and heat transfer with constant wall temperature. Kobus and Oshio [6] carried out a theoretical and experimental study on the performance of pin fin heat sinks. A theoretical model was proposed to predict the influence of various geometrical, thermal and flow parameters on the effective thermal resistance of heat sinks. Subsequently, Kobus and Oshio [7] investigated the effect of thermal radiation on the heat transfer of pin fin heat sinks and presented an overall heat transfer coefficient that was the sum of an effective radiation and a convective heat transfer coefficient.

Although many previous researches were made towards the understanding of natural convection from round pin fin arrays, nearly no experimental data are available for the pin fins having rectangular configuration which is also a very popular fin configuration used in electronic cooling applications. In particular, few researches have explicitly demonstrated the subtle difference of orientation effect on the pin fin performance, which is of practical importance for relevant applications. For this reason, the first objective of this study is to provide experimental data for square pin fin heat sinks under natural convection. Secondly, the dependence of the pin fin performance on the orientation effect is presented in a more detailed manner.

2. Experimental facility

Experiments are performed in an environmental chamber whose volume is 0.5 m × 0.5 m × 0.65 m ($L \times W \times H$). The environmental chamber can provide a temperature condition in the range of 0 °C $\leqslant T_a \leqslant$ 50 °C with a controlled resolution of 0.2 °C. To simulate the natural flow condition, the air ventilator is turned off inside the test chamber when the ambient temperature reaches 25 °C. In particular, the air conditioner outside the test chamber

continues to operate to maintain the room temperature at 25 °C. The test facility is inside the test chamber which consists of a heat sink, a heater, an insulation box, and a tilting mechanism as illustrated in Fig. 1.

The heat sinks are made of aluminum alloy 5083 with a thermal conductivity of 121 W m^{-1} K^{-1}. Seven pin fin heat sinks are made via CNC machining with a manufacture precision of 0.03 mm. The heat sinks are cleaned and tested at an ambient temperature of 25 °C with the power inputs ranging from 1 W to 18 W. Detailed dimensions of the test samples are shown in Table 1 and Fig. 2.

A Kapton heater with an identical size as the base plate of the heat sink is used to eliminate the spreading resistance. An insulation box made of bakelite with a low thermal conductivity of 0.233 W m^{-1} K^{-1} is placed beneath the heater to reduce the heat loss. In addition, a high thermal conductivity grease ($k = 2.1$ W m^{-1} K^{-1}) is used to connect the heat sink and the heater. For further minimization of the contact resistance, four M4 screws with fixed applied pressure located at the corners of the base plate are employed. The heater is powered by a DC power supply.

Each heat sink is equally equipped with nine T-type thermocouples to obtain the mean temperature of the base plate (T_b) of the heat sink. The dots shown in Fig. 1 indicate the locations of the thermocouples. The thermocouples were pre-calibrated with an accuracy of 0.1 °C. In addition, a total of 10 T-type thermocouples are installed inside the insulation box at two cross positions to calculate the heat loss from the bottom of the Kapton heater. Each cross-section is equally instrumented with five T-type thermocouples to obtain the mean temperature of that cross-section. The averaged temperature is then used to estimate the heat loss via Fourier's law of conduction. The exact total heat supply (Q_t) is then obtained by subtracting the estimated heat loss from the power input. The signals from thermocouples are then transmitted to a data acquisition system for further data reductions. Usually, each test run needs approximate 2 h to reach equilibrium when the power is turned on.

Table 1
Geometric details of tested heat sinks

	S_p (mm)	S (mm)	H (mm)	L (mm)	ψ (A_t/A_b)	ϕ (V_f/V_{ff})
Sample #1	2	8	10	100	1.758	0.952
Sample #2	2	5	10	100	2.533	0.909
Sample #3	2	3	10	100	4.032	0.829
Sample #4	2	2	10	100	6.053	0.740
Sample #5	2	2	6	100	4.032	0.740
Sample #6	2	2	4	100	3.021	0.740
Sample #7	2	2	2	100	2.011	0.740
Flat plate	–	–	0	100	1	–

3. Data reduction

In the present study, the ambient air temperature is always controlled at 25 °C and the thermophysical properties in the Nu and Ra numbers are evaluated at the film temperature, i.e.

$$T_f = \frac{1}{2}(T_a + T_b). \tag{1}$$

The average heat transfer coefficient can be calculated from the following:

$$\overline{h} = Q_C/\eta_0 A_t(T_b - T_a), \tag{2}$$

$$\overline{Nu} = \overline{h}L/\lambda, \tag{3}$$

$$Q_C = Q_t - Q_R. \tag{4}$$

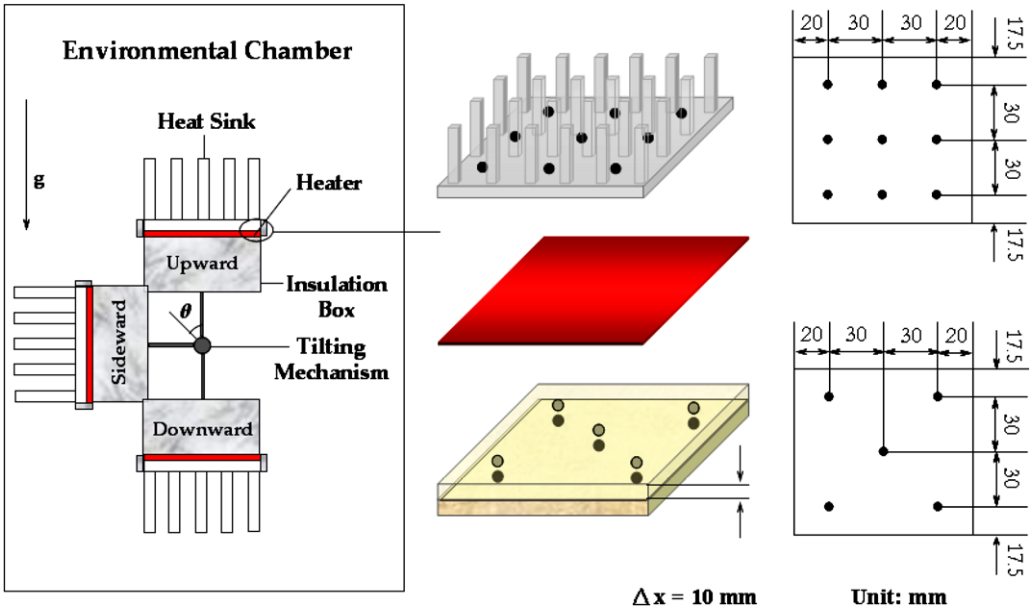

Fig. 1. Schematic of the experimental setup.

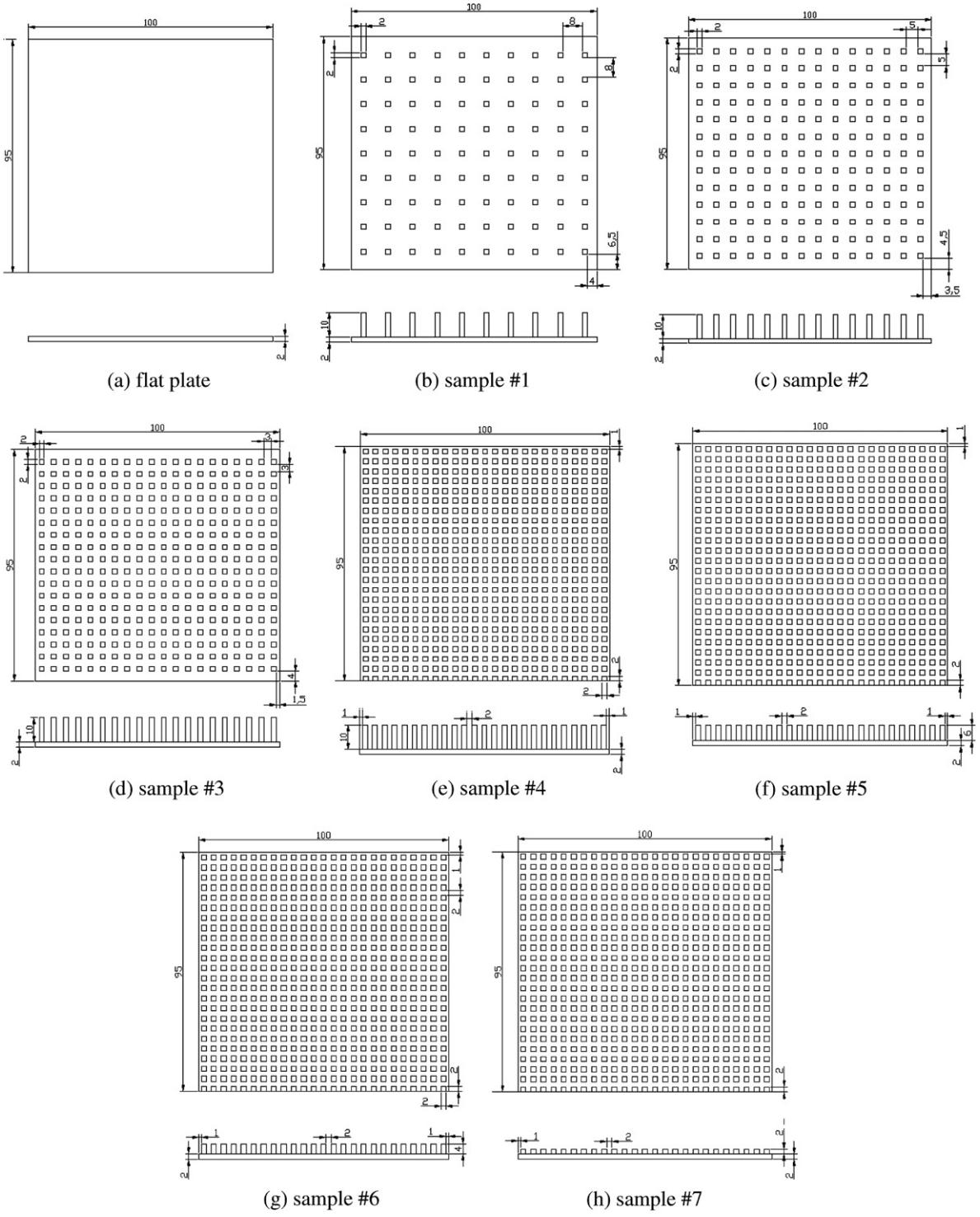

Fig. 2. Detailed geometry of test samples.

For the problem of interest, Q_t is transferred to the environment via both convection and radiation. The radiation contribution can be estimated using the following equation which describes the net heat transfer between two surfaces [8]:

$$q_{12} = \frac{\sigma(T_1^4 - T_2^4)}{\frac{1-\varepsilon_1}{\varepsilon_1 A_1} + \frac{1}{A_1 F_{12}} + \frac{1-\varepsilon_2}{\varepsilon_2 A_2}}. \quad (5)$$

Following the reducing procedure by Zografos and Sunderland [2], the radiation heat transfer is

$$q_{34} = \frac{A_4\sigma(T_3^4 - T_4^4)}{(A_4/A_3)[(1-\varepsilon_3)/\varepsilon_3 A_3] + 1}. \quad (6)$$

By subtracting the radiation contribution, the heat transferred by natural convection can be determined. To better calculate the heat transfer coefficient, one shall take into

account the overall fin efficiency (η_0). By solving Eq. (2) with iteration, the η_0 for every test sample can be obtained. The lowest η_0 encountered in the present study is around 0.99, so that η_0 is reasonably assumed unity for simplicity. The Rayleigh number is proportional to the temperature difference ($T_b - T_a$), which is the major driving potential throughout the experiments, and is expressed as

$$Ra = g\beta(T_b - T_a)L^3/\nu\alpha. \quad (7)$$

The experimental uncertainty is estimated using the uncertainty propagation equation proposed by Kline and McClintock [9]. As shown in Eq. (2), $\bar{h} = \bar{h}(Q_C, A_t, \eta_0, T_a, T_b)$, the measured uncertainties summed into the heat transfer coefficient are from the ambient air temperature, the base plate temperature, the total surface area, and the total heat supply. By substituting the measured data into the equation, the highest uncertainty for the heat transfer coefficient is about 12.82%, occurring at the lowest input power of 1 W. In particular, this uncertainty drastically decreases to less than 3% when the power input is larger than 2 W.

4. Results and discussion

For the purpose of comparison, an un-finned flat plate with the same dimension of the base plate of the test samples is used as a basic reference. The test result of this plate is first compared with the correlation given by Al-Arabi and El-Riedy [10] in the laminar region of $Ra \leqslant 4 \times 10^7$. The present result of flat plate shows a good agreement with the previous measurement as shown in Fig. 3. The heat transfer coefficients for the flat plate and the present heat sinks are shown in Figs. 4–6. Generally, the results indicate that the heat transfer coefficients for all test samples increase with the temperature difference between the base plate and the ambience. In addition, the heat transfer coefficient increases with decreasing the finning factor (ψ) which represents the total surface area divided by the base surface area (A_t/A_b).

The effect of orientation on the heat transfer coefficient is also shown in Figs. 4–6. In essence, the downward facing orientation yields the lowest heat transfer coefficient. However, one can notice that the heat transfer coefficients for upward and sideward facing orientations are of comparable magnitude. For the flat plate, sample #1, sample #2, and sample #7, the heat transfer coefficients for sideward arrangement are higher than those for upward arrangement. By contrast, the other test samples (samples #3–#6) show an opposite trend. At first sight, this finding looks contradictory as compared with that by Sparrow and Vemuri [1] who conducted experimental study on round pin fin arrays and concluded that the upward facing orientation gave the highest heat transfer rates, followed by the sideward facing and the downward facing ones. As we further examine this qualitative difference, both results turn out to be reasonable. This phenomenon can be associated with the induced plumes. For the un-finned plate with the sideward arrangement, the buoyancy-induced flow is mainly from the bottom of the plate surface; however, this induced air flow comes from the four edges of the plate for the upward arrangement as illustrated in Fig. 7 [11]. Analogous flow pattern is applicable to the finned surface, hence one can expect that finning has a greater influence on the sideward arrangement than on the upward arrangement since it blocks some air flow and acts as a flow barrier

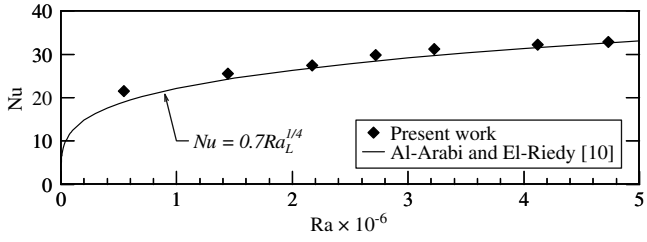

Fig. 3. Comparison of present results of the flat plate with the correlation given by Al-Arabi and El-Riedy [10].

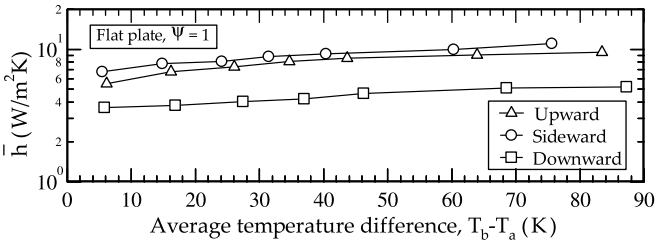

Fig. 4. Heat transfer performance of the flat plate for all three orientations.

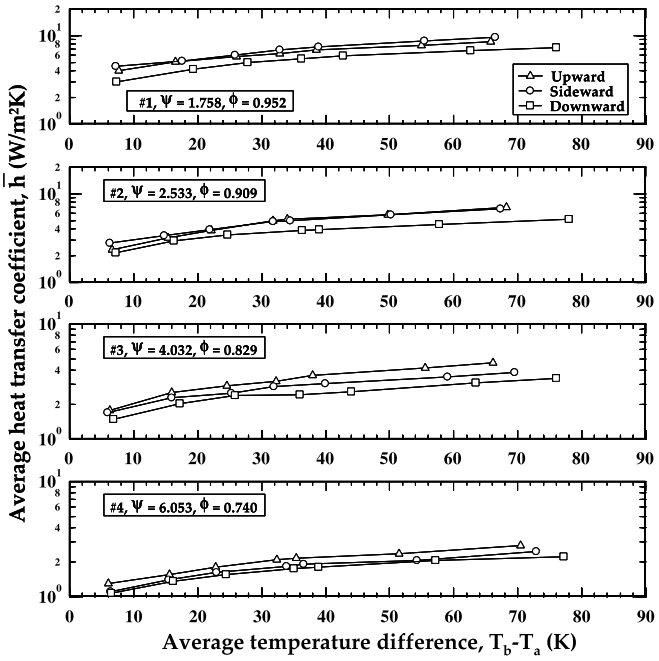

Fig. 5. Heat transfer performance of samples #1–#4 for all three orientations.

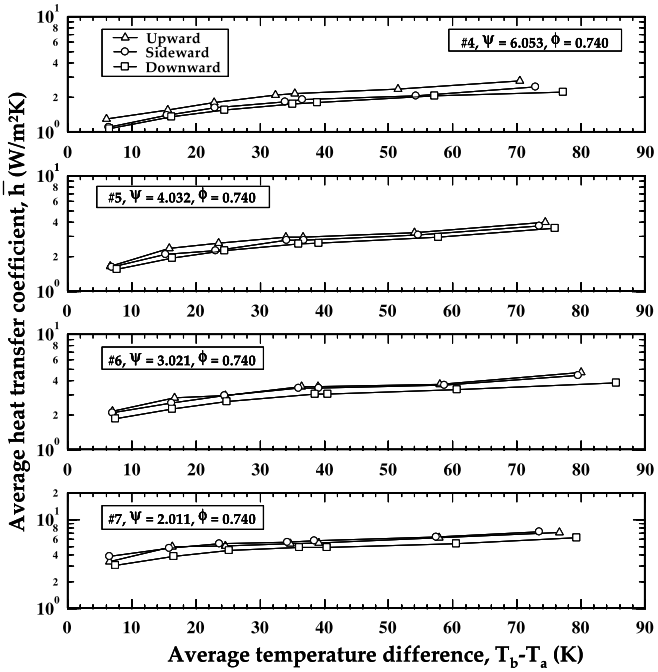

Fig. 6. Heat transfer performance of samples #4–#7 for all three orientations.

for the sideward arrangement. With the further increase in fin surface, the flow pattern for upward arrangement remains similar while the sideward arrangement experiences a dramatic change that the main flow arrived at the bottom of the heat sink is blocked when the induced air flow penetrates through the fins as depicted in Fig. 8b. A similar flow pattern was also observed by Aihara et al. [3]. For the problem of interest, a threshold may exist beyond which the sideward arrangement is surpassed by the upward arrangement. The comparison among three orientations for varied finning factor is shown in Fig. 9. With the finning factor being varied from 1.0 to 6.053 for the upward and sideward arrangements, the performance of sideward arrangement initially takes the lead, matches that of upward arrangement at $\psi = 2.7$, and is overtaken thereafter. As clearly seen in this figure, the performance of sideward arrangement may be superior or inferior to that of upward arrangement by 20% at $\psi = 1.0$ and $\psi = 6.053$, respectively. Similarly, the performance of sideward arrangement gradually approaches that of downward arrangement when the finning factor increases. In fact, the performance of sideward arrangement surpasses that of downward arrangement by more than 120% at $\psi = 1.0$ and is only 8% higher at $\psi = 6.053$.

Aside from the finning factor, the pin fin performance is also found to be related to the heat sink porosity (ϕ) which is defined as the volume fraction of fluid inside the heat sink (V_f/V_{ff}). This factor is regarded as a measure of the inner drag of the heat sink. According to the flow pattern depicted in Fig. 8, increasing the heat sink porosity is advantageous to both upward and sideward arrangements since it promotes the penetration depth of the ventilation. This may explain the fluctuation behavior of the profile ($\overline{h}_{downward}/\overline{h}_{sideward}$) in which sample #2 is lower than sample #7 and sample #3 is lower than sample #5. As we examine

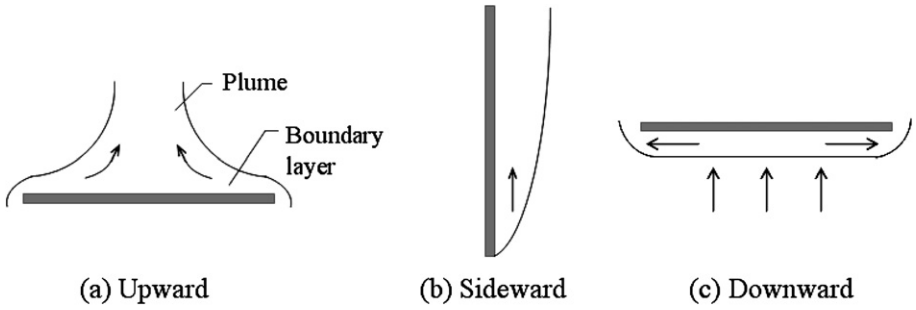

Fig. 7. Schematic of induced main flow for a flat plate subject to three orientations [11].

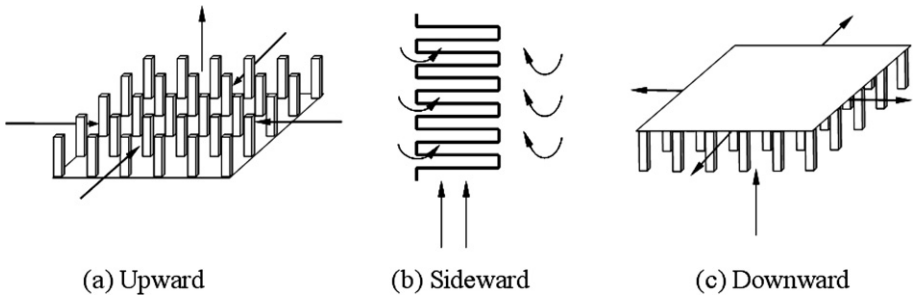

Fig. 8. Schematic of induced main flow for pin fin geometry subject to three orientations.

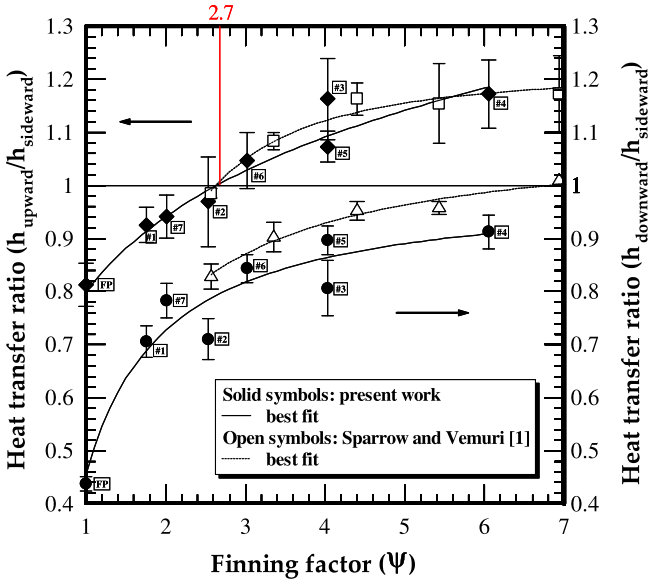

Fig. 9. Comparison among three orientations for varied finning factor.

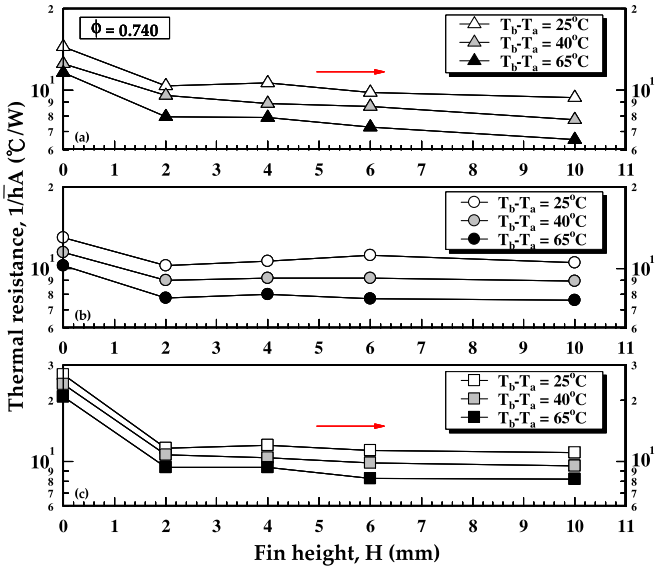

Fig. 10. Dependence of the thermal resistance on the fin height, (a) upward, (b) sideward, and (c) downward.

the staggered pin fin arrays tested by Sparrow and Vemuri [1], the corresponding finning factors are 2.571, 3.356, 4.403, 5.431, and 6.934, respectively. Although the smallest one is below 2.7, the presence of staggered arrangement inevitably contributes the flow resistance and reduces the performance for sideward arrangement, thus rendering the upward arrangement to prevail throughout their study. In addition, for the staggered arrangement having $\psi = 6.934$ and $\phi = 0.37$, the most dense sample in their study shows almost identical performance between the sideward and downward arrangements.

The dependence of the thermal resistance subject to the influence of the fin height is shown in Fig. 10. For a fixed porosity of 0.74, the thermal resistance for upward and downward arrangements continues to decrease with the rise of fin height. This result indicates that, even if the induced convection becomes less effective with the fin height, the enhancement of surface area still outweighs the reduction of heat transfer coefficient. Nevertheless, for sideward arrangement, the thermal resistance becomes independent of the fin height when the fin height is greater than 2 mm. The advantage of increased surface area is offset by the decrease of heat transfer coefficient can be attributed to the choking phenomenon occurring among the pin fins as proposed by Zografos and Sunderland [2]. The rising air flow within the heat sink is termed choked due to a balance of viscous drag and buoyancy force. The dependence of thermal resistance on the heat sink porosity is shown in Fig. 11. For a fixed fin height of 10 mm, the optimal porosity for upward arrangement is around 0.83 while that for sideward arrangement is around 0.91. The optimal porosity for sideward arrangement occurs at a higher value due to its sensitive nature of performance associated with the fin configuration. In particular, one can notice that the thermal resistance consistently decreases with reducing

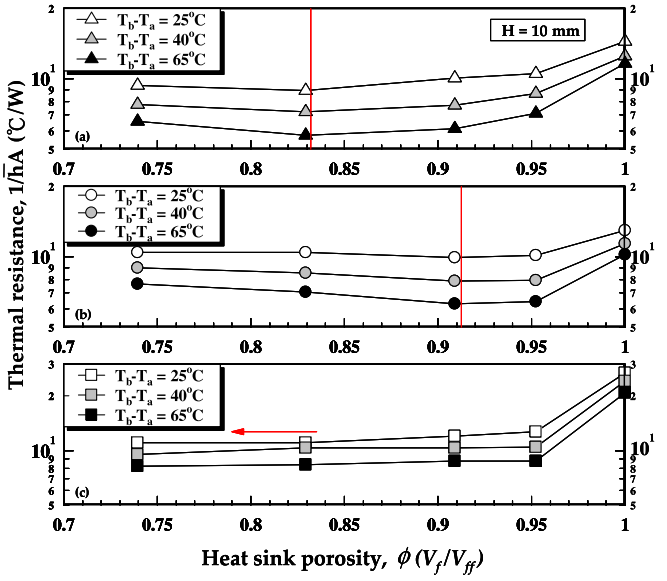

Fig. 11. Dependence of the thermal resistance on the heat sink porosity, (a) upward, (b) sideward, and (c) downward.

the heat sink porosity at downward arrangement over the test range of $0.74 \leqslant \phi \leqslant 1.0$. This result, once again, suggests that finning is comparatively effective for downward arrangement.

To further examine the effect of finning on heat transfer performance, the augmentation factor (ξ), which represents the augmented heat transfer of a heat sink relative to that of a flat plate, is proposed as follows:

$$\frac{(\bar{h}A)_{hs}}{(\bar{h}A)_{fp}} = \xi = f(Ra_L, \psi, \phi, \theta). \tag{8}$$

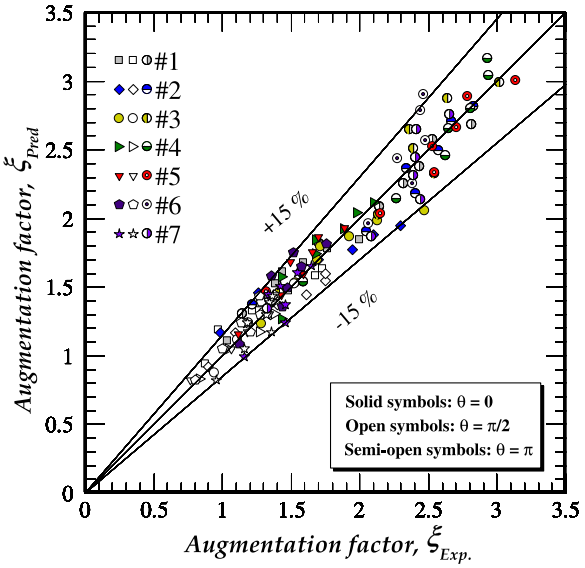

Fig. 12. Comparison between the proposed correlation and experimental data.

Employing the multi-regression analysis, the augmentation factor is empirically correlated by the following equation:

$$\xi = (0.0423 - 0.00493\theta^{1.5})Ra_L^{(0.244+0.0051\theta^{2.5})} \times (\psi)^{(0.125-0.157\theta+0.05\theta^2)}(\phi)^{(0.557-0.0192\theta^3)} \quad (9)$$

with a mean deviation of 6% and a standard deviation of 8%. Fig. 12 shows the comparison between the experimental data and those predicted by Eq. (9). The accuracy of this correlation is generally within 15%. Generally, from $\theta = 0$–π, the augmentation factor increases with the Rayleigh number but shows intricate dependence with the finning factor and the heat sink porosity. One can also see that the augmentation factor is around 1.1–2.5 for upward arrangement (solid symbols), around 0.8–1.8 for sideward arrangement (open symbols), and around 1.2–3.2 for downward arrangement (semi-open symbols). For a highly finned surface at sideward arrangement, the augmentation factor may slightly be less than unity at a lower Rayleigh number. Part of the reasons is because the flow pattern is more sensitive to the fin structure, and the heat transfer coefficient of the flat plate is relatively higher at this orientation.

5. Conclusions

The heat transfer characteristics of square pin fin heat sinks subject to the influence of orientation are examined under natural convection in the present study. Based on the foregoing discussion, the following conclusions are made:

1. Generally, the downward facing orientation yields the lowest heat transfer coefficient. However, the heat transfer coefficients for upward and sideward facing orientations are of comparable magnitude. It is found that the performance of sideward arrangement exhibits a greater dependence on fin structure. The sideward arrangement outperforms the upward one for small finning factors of $\psi \leqslant 2.7$, beyond which the situation is reversed.
2. The performance of sideward arrangement may be superior or inferior to that of upward arrangement by 20% at $\psi = 1.0$ and $\psi = 6.053$, respectively. In addition, with a gradual increase in finning factor, the performance of sideward arrangement approaches that of downward arrangement. The performance of sideward arrangement surpasses that of downward arrangement by 120% at $\psi = 1.0$ and only by 8% at $\psi = 6.053$.
3. The optimal heat sink porosity is around 0.83 for the upward arrangement and is around 0.91 for the sideward arrangement. In particular, finning is generally more effective for downward arrangement throughout the present study regardless of the finning factor and the heat sink porosity.
4. The pin fin arrays in the present study outperform the flat plate on the thermal performance by 1.1–2.5 times for upward arrangement, by 0.8–1.8 times for sideward arrangement, and by 1.2–3.2 times for downward arrangement. It is found that finning is comparatively more effective for downward arrangement and is less effective for sideward arrangement.

Acknowledgements

This work was supported by the National Science Council of Taiwan under contract of NSC 95-ET-7-007-003-ET and the supporting funding from the Department of Industrial Technology, Ministry of Economic Affairs, Taiwan. The authors thank Mr. C.T. Huang for his help during experimental setup.

References

[1] E.M. Sparrow, S.B. Vemuri, Orientation effects on natural convection/radiation heat transfer from pin-fin arrays, Int. J. Heat Mass Transfer 29 (3) (1986) 359–368.
[2] A.I. Zografos, J.E. Sunderland, Natural convection from pin fin arrays, Exp. Therm. Fluid Sci. 3 (1990) 440–449.
[3] T. Aihara, S. Maruyama, S. Kobayakawa, Free convective/radiative heat transfer from pin fin arrays with a vertical base plate (general representation of heat transfer performance), Int. J. Heat Mass Transfer 33 (6) (1990) 1223–1232.
[4] T.S. Fisher, K.E. Torrance, Free convection limits for pin-fin cooling, J. Heat Transfer 120 (3) (1998) 633–640.
[5] K. Park, D.H. Choi, K.S. Lee, Optimum design of plate heat exchanger with staggered pin fin arrays, Numer. Heat Transfer A 45 (4) (2004) 347–361.
[6] C.J. Kobus, T. Oshio, Development of a theoretical model for predicting the thermal performance characteristics of a vertical pin-fin array heat sink under combined forced and natural convection with impinging flow, Int. J. Heat Mass Transfer 48 (6) (2005) 1053–1063.
[7] C.J. Kobus, T. Oshio, Predicting the thermal performance characteristics of staggered vertical pin fin array heat sinks under combined

mode radiation and mixed convection with impinging flow, Int. J. Heat Mass Transfer 48 (13) (2005) 2684–2696.
[8] J.P. Holman, Heat Transfer, McGraw-Hill, Singapore, 1989, p. 402.
[9] S.J. Kline, F.A. McClintock, Describing uncertainties in single-sample experiments, Mech. Eng. 75 (1953) 3–8.
[10] M. Al-Arabi, M.K. El-Riedy, Natural convection heat transfer from isothermal horizontal plates of different shapes, Int. J. Heat Mass Transfer 19 (12) (1976) 1399–1404.
[11] A. Bejan, Convection Heat Transfer, second ed., Wiley, New York, 1995, p. 196.